EurJIC
European Journal of Inorganic Chemistry

Chemistry Europe
European Chemical Societies Publishing

Accepted Article

Title: Supported Ionic Liquids for the Efficient Removal of Acetylsalicylic Acid from Aqueous Solutions

Authors: Sandra C. Bernardo, Beatriz R. Araújo, Ana C.A. Sousa, Rafael A. Barros, Ana C. Cristovão, Márcia C. Neves, and Mara Guadalupe Freire

To be cited as: *Eur. J. Inorg. Chem.* 10.1002/ejic.202000101

Link to VoR: https://doi.org/10.1002/ejic.202000101

WILEY-VCH

WILEY-VCH

FULL PAPER

Supported Ionic Liquids for the Efficient Removal of Acetylsalicylic Acid from Aqueous Solutions

Sandra C. Bernardo[a], Beatriz R. Araújo[a], Ana C.A. Sousa[a], Rafael A. Barros[b], Ana C. Cristovão[b], Márcia C. Neves[a] and Mara G. Freire[a]*

[a] CICECO – Aveiro Institute of Materials and Department of Chemistry
University of Aveiro
Campus Universitário de Santiago, 3810-193 Aveiro, Portugal
E-mail: maragfreire@ua.pt
[b] CICS-UBI – Health Sciences Research Centre,
University of Beira Interior,
Av. Infante D. Henrique, 6200-506 Covilhã, Portugal

Abstract: Acetylsalicylic acid, commercially available as aspirin, is one of the most used drugs in the world, being detected in several environmental compartments, including drinking water supplies. Given its environmental impact, the development of a cost-effective technology capable of removing this pharmaceutical from water samples is of high relevance, for which materials based on silica chemically modified with ionic liquids (SILs) can be foreseen as a promising alternative. In this work, four SILs (with the chloride anion and imidazolium or tetraalkylammonium cations of different alkyl side chain length) were synthesized and characterized, and their potential for the adsorption of acetylsalicylic acid appraised by adsorption kinetics and isotherms. Envisioning their use to treat drinking water, the toxicity of all SILs towards the liver cell line Hep2G was determined. The best identified SIL, comprising the dimethylbutylammonium cation, displays a maximum adsorption capacity of 0.08 mmol/g, being 1 g of this material sufficient to treat ca. 14,500 L of water containing 1 µg/L of acetylsalicylic acid (under ideal conditions). Furthermore, this material has a negligible toxicity towards the liver cell line Hep2G. The results obtained reinforce the potential of SILs as alternative adsorbents to effectively remove acetylsalicylic acid from aqueous solutions, and may be envisioned as a promising strategy for the treatment of wastewater and drinking water.

Introduction

Pharmaceutical drugs are widely used due to the worldwide continuous growing population and advances in the health-care sector. However, they also significantly contribute to environmental pollution and pose secondary health risks[1–4]. Pharmaceuticals are not fully metabolized upon administration, being excreted by patients and reaching the aquatic environment[2,5–8]. Over 630 pharmaceuticals have been detected in the environment[1], with concentrations in effluents from wastewater treatment plants (WWTP) ranging from ng/L to mg/L[9]. Although the environmental and health risks of active pharmaceutical ingredients (APIs) remain to be fully understood, specially due to the unknown chronic effects on humans[10,11], it is known that some of these compounds exert cytotoxic, genotoxic, mutagenic, carcinogenic and/or teratogenic effects[11]. Furthermore, there are still data gaps in what concerns their ecotoxicological effects, and even less is known on synergistic effects of pharmaceuticals mixtures, together with their human metabolites and degradation products[2,11,12]. Not only the parent drugs raise concerns to the environment, but also their pharmacologically active metabolites and/or transformation products, formed during water treatment or under environmental conditions, might have a negative impact on aquatic biota[2,10,13]. Overall, it is clear that there is a significant demand to reduce the input and presence of drugs in the water cycle and in the environment[2,12,14].

The most frequently detected pharmaceuticals in wastewater are acetylsalicylic acid, diclofenac, ibuprofen, naproxen, paracetamol and phenazone[1]. Average values of these drugs in WWTP effluents range between 160 and 810 ng/L, but maximum concentrations as high as 0.6-6.0 mg/L have been registered[15]. In order to reduce the levels of pharmaceuticals in wastewaters, various treatment technologies can be applied, including biological treatment, ozonation, UV irradiation and advanced oxidation processes, such as ozonation/H_2O_2, UV/H_2O_2 and UV/TiO_2[13,16–19]. Nevertheless, some studies have shown that ozone is an unfavorable oxidant[16] and (photo)oxidation processes may produce more toxic or recalcitrant by-products[2]. Advanced treatment of effluents has been investigated using membrane filtration[12,17], powdered charcoal[12,16], and constructed wetlands[20]. In addition to scarce, the reported techniques for the removal of drugs in wastewaters have some drawbacks and some are difficult to implement in wastewater treatment plants[2,21].

Supported ionic liquids (SILs) have been described as alternative materials for solid-phase extraction (SPE)[22–25]. Ionic liquids (ILs) are organic salts, usually constituted by an organic cation (e.g. imidazolium, pyridinium, pyrrolidium, tetraalkylammonium and tetraalkylphosphonium) paired with organic or inorganic anions (e.g. trifluoromethylsulfonate, bis(trifluoromethylsulfonyl)imide, hexafluorophosphate, trifluoroethanoate, tetrafluoroborate, Cl^-, Br^- and I^-)[22–29]. Amongst the interesting features of neat ILs, such as negligible volatility, high thermal stability and high polarity[22], the most interesting characteristic is their tunability. ILs can be tailored to display a set of specific physicochemical properties by changing the cation/anion chemical structure, being a property transferrable to SILs. In SPE, ILs/SILs can be designed to promote specific interactions between the target compound and the adsorbent, allowing higher adsorption efficiencies and increased selectivity when dealing with complex matrices[23]. Accordingly, several works can be found in the literature with ILs covalently bound to materials (SILs) or physically immobilized on polymeric supports (known as supported IL phases – SILPs)[25]. SILPs as SPE materials for the removal of drugs from aqueous media emerged in 2009, when Fontanals et al.[22] proposed the use of crosslinked polymer-supported imidazolium

trifluoroacetate salt for the removal of APIs from different water samples, with the complete recovery of the studied compounds [22]. More recently, different anions were used to prepare polymer-supported imidazolium-based ILs, namely trifluoromethanesulphonate ($[CF_3SO_3]^-$) and tetrafluoroborate ($[BF_4]^-$)[30]. The previously synthesized SILP[22] was used for comparison with these new SILPs as potential adsorbents for several acidic compounds from aqueous samples[30]. Regarding silica-based SILs one of the first reports dates from 1985, where silica gel was functionalized with 3-(1-imidazolyl)propyl groups to adsorb and preconcentrate metal ions from ethanol solutions[31]. However, it was only after 2004, after the work of Jiang's research group[32], that the use of ILs immobilized onto silica supports for SPE has become more popular. SILS based on silica have been mainly used to separate small molecules from natural extracts and metals[25].

Herein we demonstrate the synthesis of a novel series of SILs based on silica, with the common chloride anion and different cations, and investigate their application as adsorbents to remove pharmaceuticals from water. To this end, acetylsalicylic acid, commercially sold as aspirin, was used. Aspirin is a non-steroidal anti-inflammatory drug and it is one of the most commonly used pharmaceuticals in the world[33,34]. Moreover, acetylsalicylic acid is one of the drugs that upon transformation becomes more toxic, since it is easily degraded by deacetylation into its more active form, salicylic acid, which has a higher logK_{ow} and a lower half maximal effective concentration (EC_{50})[35]. Therefore, removal methods for this API should be used instead of treatment methods. Maximum concentrations of 1.51 µg/L and 13 ng/L of acetylsalicylic acid were detected in sewage/effluents and in drinking water, respectively[35–37]. Furthermore, high levels of the acetylsalicylic acid metabolite, salicylic acid, were detected in hospital wastewaters in Greece (> 2 mg/L)[38] and industrial wastewaters (>3 mg/L) in Spain[39], whereas average concentrations of 295 ng/L and 70 ng/L were registered in Spanish river waters and WWTP influents, respectively[40]. In Portugal, salicylic acid was detected at levels ranging from 1.17 to 61.26 µg/L in WWTPs influents and from 0.11 to 0.30 µg/L in effluents[41]. Salicylic acid was also found in tap water and mineral waters from Spain with average values of 31 ng/L and 33 ng/L[40]. Given its negative impact on the environment, several materials have been tested for the removal of acetylsalicylic acid from aqueous solutions, such as natural clays (kaolin and bentonite), a natural zeolite (clinoptilolite), and activated carbon[42,43]. Previously, we synthesized other SILs, namely imidazolium-based SILs with different anions, and demonstrated their remarkable potential as alternative adsorbents to remove diclofenac from aqueous media[44]. The previous results allowed to conclude that SILs comprising the chloride counterion are more effective as adsorbents for APIs[44]. Accordingly, in this work, three novel SILs containing the chloride anion and quaternary ammoniums with different alkyl side chain length as cations were synthesized and characterized, and their performance as acetylsalicylic acid adsorbents studied. The previously best identified SIL[44], was also investigated herein for comparison purposes. Adsorption kinetics and isotherms experimental data were obtained for acetylsalicylic acid onto all SILs, and several models were applied to fit the experimental data. Additionally, and envisaging the application of these SILs as alternative adsorbents to treat drinking water, we evaluated their cytotoxicity towards the liver cell line Hep2G, a well-established model for cytotoxicity evaluation.

Results and Discussion

Preparation and characterization of SILs

Scheme 1 presents a schematic overview of the SILs synthesis procedure and different reagents used as cation source, as well as the SILs abbreviation. Although different cation sources have been investigated, chloride was kept as the counterion in all SILs. The use of chloride instead of other more complex anions was proven to be advantageous for the removal of diclofenac by us in a previous work[44], while lowering the cost of the materials and reducing their eco- and cytotoxicity by avoiding the use of more complex and organic anions. Overall, three new SILs were prepared in this work ($[Si][N_{3114}]Cl$, $[Si][N_{3444}]Cl$, and $[Si][N_{3888}]Cl$), being investigated in terms of their performance for the removal of acetylsalicylic acid from aqueous media. The SIL previously reported by us[44] based on an imidazolium cation ($[Si][C_3C_1Im]Cl$) was used for comparison purposes.

All SILs were prepared by a two-step reaction process, summarized in Scheme 1, where activated silica particles react first with a silane-coupling agent (3-chloropropyltrimethoxysilane) and the obtained chloropropylsilica reacts with N-methylimidazole or other tertiary ammines as the cation source. The synthesis procedure was adapted from Qiu et al.[45], although a novel synthesis approach is shown in this work by including other tertiary ammines not based on imidazole.

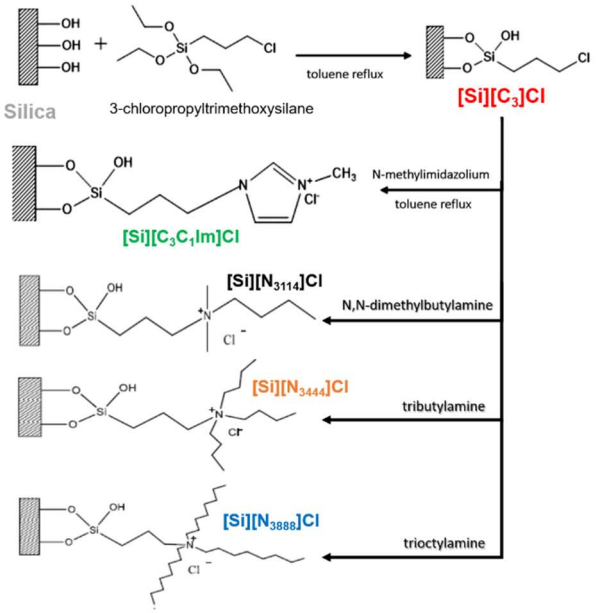

Scheme 1. Schematic representation of the preparation of SILs, their chemical structures and respective abbreviations. Enclosed is represented chloropropylsilica, which is the intermediate of the two-step reaction.

Elemental analysis was carried out to quantitatively determine the carbon, hydrogen, and nitrogen contents of the prepared SILs, whose results are provided in Table 1. The carbon and nitrogen contents (in percentage weight fraction) range from 4.64% to 12.14% and from 0.07% to 2.84%, respectively. It should be noted that no nitrogen was detected in $[Si][C_3]Cl$, the intermediate material of the two-step reaction, supporting the absence of IL organic moieties. On the other hand, the presence of nitrogen, carbon and hydrogen demonstrate that the studied ILs were successfully covalently attached to the silica surface. The Fourier-transform infrared spectroscopy (FTIR) spectra of activated silica,

chloropropyl silica, and prepared SILs were also acquired, being given in Figure S2 in the Supporting Information, further confirming the silica functionalization by ILs.

Table 1. C, H and N weigh fraction percentage, Brunauer-Emmett-Teller (BET) specific surface area, and IL bonding amount on SILs.

SIL	% C	% H	% N	BET (m^2/g)	Bonding amount (μmol/m^2)	Bonding amount (mmol/g)
silica	--	--	--	434.6	--	--
[Si][C_3]Cl	4.637	1.394	--	322.9	--	--
[Si][C_3C_1Im]Cl	8.382	2.120	2.841	185.3	2.617	1.015
[Si][N_{3114}]Cl	7.719	1.840	0.767	187.1	1.409	0.548
[Si][N_{3444}]Cl	5.741	1.336	0.148	323.4	0.262	0.106
[Si][N_{3888}]Cl	6.899	1.335	0.071	299.2	0.128	0.051

The bonding amount of ILs onto SILs was determined from the elemental analysis data (details of the equations for this type of calculations are given in the Supporting Information). For these calculations, the specific surface area (S_{BET}) of the initial silica (434.6 m^2/g) was used. The higher number of IL functional groups appears in the [Si][C_3C_1Im]Cl material, followed by [Si][N_{3114}]Cl, [Si][N_{3444}]Cl, and [Si][N_{3888}]Cl, with values decreasing from 1.015 to 0.051 mmol/g. These values are relevant to appraise the materials performance to adsorb acetylsalicylic acid, as discussed below.

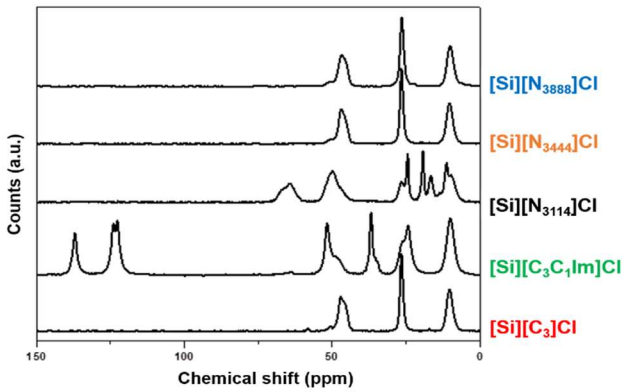

Figure 1. Solid-state ^{13}C NMR spectra of [Si][C_3]Cl and SILs.

The successful preparation of SILs was additionally confirmed through solid-state ^{13}C Nuclear magnetic resonance (NMR), whose spectra are shown in Figure 1. Concerning the [Si][C_3]Cl spectrum, three peaks at 10, 27 and 47 ppm are assigned to the three carbons of the propyl alkyl chain. For the [Si][C_3C_1im]Cl, the carbon peaks of the imidazolium ring at 122 and 137 ppm, of the methyl chain at 37 ppm, and of the propyl chain at 10, 24 and 52 ppm are identified. The spectrum of [Si][N_{3114}]Cl shows the peaks assigned to the carbons of the propyl chain at 11, 24 and 67 ppm, the carbon of the methyl chain at 50 ppm and lastly the carbons of the butyl chain, at 17, 19, 25 and 63 ppm (peaks assignment is shown in the Supporting Information, Figure S1). On the other hand, the solid-state ^{13}C NMR spectra of [Si][N_{3444}]Cl and [Si][N_{3888}]Cl are similar to the spectrum of the starting material ([Si][C_3]Cl), which is due to the lower functionalization degree of these materials, being in agreement with the elemental analysis results and IL bonding amount provided in Table 1.

Zeta potential measurements were performed to study the surface charge of the functionalized silica-based materials. Data of the zeta potential as a function of pH for the synthesized SILs and [Si][C_3]Cl are provided in the Supporting Information (Figure 3). From these data, it was determined the point of zero charge (PZC), which is the pH value at which a solid particle in suspension exhibits zero net electrical charge on its surface. Table 2 provides the PZC values of the prepared SILs. All four synthesized SILs display higher PZC values than [Si][C_3]Cl and the starting silica, confirming the presence of a cation in SILs and the successful silica functionalization.

Table 2. Point zero charge values of silica, [Si][C_3]Cl and SILs.

SIL	PZC
silica	3.4
[Si][C_3]Cl	4.1
[Si][C_3C_1Im]Cl	9.5
[Si][N_{3114}]Cl	9.2
[Si][N_{3444}]Cl	7.4
[Si][N_{3888}]Cl	6.2

Finally, Scanning Electron Microscopy (SEM) was used to address the morphology of the prepared materials. Figure 2 depicts the SEM images of starting silica and [Si][N_{3114}]Cl. SEM images for the remaining SILs are given in the Supporting Information (Figure S4). Overall, no significant differences in the materials morphology is observed between the prepared SILs and the non-functionalized silica, meaning that the silica functionalization with ILs and required reaction steps do not change the material morphology.

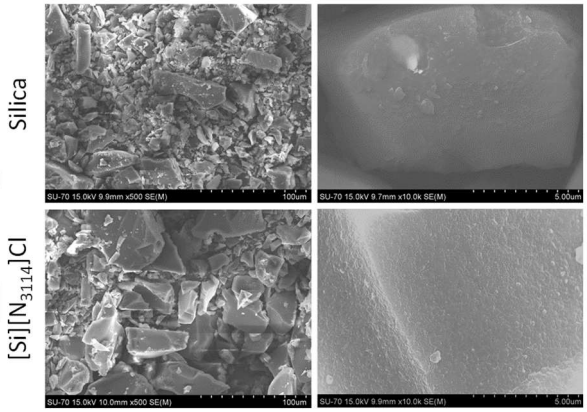

Figure 2. SEM images of silica and [Si][N_{3114}]Cl.

Adsorption kinetics, diffusion models and isotherms of acetylsalicylic acid onto SILs

The synthesized SILs were investigated as adsorbents for pharmaceuticals, while envisaging their use in the treatment of water. Acetylsalicylic acid was chosen as the target pharmaceutical since it is the most frequently used non-steroidal anti-inflammatory drug[33,34]. Furthermore, concentrations of 1.51 µg/L and 13 ng/L of acetylsalicylic acid were detected in sewage/effluents and in drinking water, respectively[35–37]. The adsorption experiments carried out include adsorption kinetics and adsorption isotherms. The adsorption kinetic curves were determined to evaluate and establish the time needed for equilibrium. For these assays, the initial acetylsalicylic acid concentration was set at 0.178 mmol/L, using 0.064 g of material and a volume of 10 mL of aqueous solution. The results obtained are depicted in Figure 3. Detailed data are given in the Supporting Information (Tables S1-S4). The experimental values of q_e, which give the equilibrium concentration of adsorbate in the solid phase (mmol/g), as well as those of the adsorption efficiency (%AE) at the conditions tested, are given in Table 3.

Table 3. Adsorption kinetics values of maximum equilibrium concentration of adsorbate in the solid phase (mmol/g) and adsorption efficiency (% AE) at 25°C.

SILs	q_e, experimental (mmol/g) ± σ	% AE ± σ
[Si][C_3C_1Im]Cl	0.0044 ± 0.0001	14.0 ± 8.7
[Si][N_{3114}]Cl	0.0232 ± 0.0016	63.5 ± 0.1
[Si][N_{3444}]Cl	0.0157 ± 0.0004	55.9 ± 3.2
[Si][N_{3888}]Cl	0.0149 ± 0.0014	53.0 ± 0.1

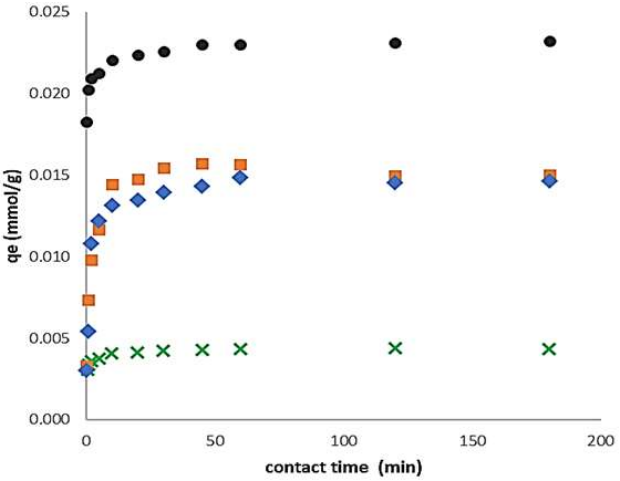

Figure 3. Adsorption kinetic curves of acetylsalicylic acid onto SILs at 25°C: ×, [Si][C_3C_1Im]Cl; ●, [Si][N_{3114}]Cl; ■, [Si][N_{3444}]Cl; ◆, [Si][N_{3888}]Cl.

Under the evaluated conditions, it is found a plateau in the equilibrium concentration of adsorbate in the solid phase (q_e) after 20 min, being constant afterwards and up to the total time considered (180 min). Thus, the adsorption of acetylsalicylic acid onto SILs is a fast process (≈ 20 min). According to Figure 3, the equilibrium concentration of adsorbate in the solid phase decreases in the following sequence of SILs: [Si][N_{3114}]Cl > [Si][N_{3444}]Cl > [Si][N_{3888}]Cl > [Si][C_3C_1Im]Cl. Moreover, the best identified material, [Si][N_{3114}]Cl, allows a maximum equilibrium concentration of adsorbate in the solid phase of 0.0232 mmol/g and an adsorption efficiency of 63.5 ± 0.1 %. It should be noted that non-functionalized silica was also tested under the same conditions. Although with a higher specific surface area (BET of 434.6m^2/g) and a similar pore size diameter, and even for a longer time tested (up to 24h), no adsorption of acetylsalicylic acid was verified on silica, at least up to the detection limit of the analytical equipment used, meaning that the IL functionalization plays a significant role on the adsorption.

Although leaching of the IL was not expected since the IL cation is covalently linked to silica and several washing steps were applied before the SILs application, the possible release or leaching of the IL from the material was appraised, both by chloride and imidazolium quantification. Numerous control assays only with SILs and water (no API added) were prepared during the kinetic studies, and no leaching of the IL containing the imidazolium aromatic ring or of chloride as the counter-ion was observed. Therefore, the SILs used are stable at the conditions applied.

To the experimental results obtained, the pseudo first-order and pseudo second-order kinetic models by Lagergren's[46] first-order rate equation (Equation I) and the Ho's[47] second-order rate equation (Equation II) were applied:

$$\ln(q_e - q_t) = \ln q_e - k_1 t \quad \text{(I)}$$

$$\frac{t}{q_t} = \frac{1}{k_2 q_e^2} + \frac{1}{q_e} t \quad \text{(II)}$$

where t is the time (min), q_e is the amount of acetylsalicylic acid adsorbed onto the adsorbent at equilibrium (mmol/g), q_t is the amount of adsorbate adsorbed onto the adsorbent at different times (mmol/g), k_1 (1/min) is the rate constant of the pseudo first-order adsorption, and k_2 (g/mmol.min) is the rate constant of the pseudo-second-order adsorption.

The adsorption kinetic parameters are summarized in Table 4, and the respective fitting curves are shown in the Supporting Information, Figure S5. The fitting of the data for all models was performed using the GraphPad Prism8 software.

According to the correlation coefficients (R^2) obtained for both kinetic models, it is shown that the pseudo second-order model better describes the adsorption experimental data (higher R^2 values), suggesting that the adsorption process is controlled by the adsorption at the liquid-solid interface in the adsorbent[47,48].

Table 4. Parameters of the pseudo first-order and pseudo second-order kinetic models.

SILs	Pseudo first-order model			Pseudo second-order model		
	q_e (mmol/g)	k_1 (1/min)	R^2	q_e (mmol/g)	k_2 (g/mmol.min)	R^2
[Si][C_3C_1Im]Cl	0.0041	2.352	0.947	0.0042	1038	0.980
[Si][N_{3114}]Cl	0.0223	3.183	0.984	0.0227	339.4	0.996
[Si][N_{3444}]Cl	0.0150	0.517	0.975	0.0157	47.32	0.989
[Si][N_{3888}]Cl	0.0141	0.558	0.980	0.0149	51.250	0.978

The diffusion process can be controlled by one or several combined steps: film diffusion, pore diffusion, surface diffusion and sorption in the pore surface. To evaluate the rate limiting process, the most usual diffusion models, namely the Boyd's film diffusion (Eq. III and Eq. IV) and the Webber's pore diffusion (Eq. V) models[49–52] were applied:

$$Bt = -0.4977 - \ln(1 - F(t)), for\ F\ values > 0.85 \quad \text{(III)}$$

$$Bt = \left(\sqrt{\pi} - \sqrt{\pi - \frac{\pi^2 F(t)}{3}}\right)^2, for\ F\ values > 0.85 \quad \text{(IV)}$$

$$q_t = K_{id} t^{1/2} \quad \text{(V)}$$

where $F(t)$ is the fractional attainment of equilibrium at different times t ($F(t) = q_t/q_e$) and Bt is a function of $F(t)$, q_t and q_e are the acetylsalicylic acid adsorbed onto the adsorbent (mmol/g) at time t and at equilibrium, respectively, and K_{id} is the internal diffusion rate constant (mmol/g.$min^{1/2}$).

The numerical results of the piecewise linear regression (PLR) applied to the experimental kinetic data obtained with the synthetized SILs are provided in Table 5. The intercept of the first linear segment in the Boyd's plot is 0.0002, 0.0068, 0.0005 and -0.0007 for [Si][C_3C_1Im]Cl, [Si][N_{3114}]Cl, [Si][N_{3444}]Cl, and [Si][N_{3888}]Cl respectively, whose confidence interval of the intercept (with 95% confidence limits) includes zero. These results suggest that under the experimental conditions applied film diffusion does not control the adsorption process during the initial period.

The numerical results for Webber' plots obtained for the adsorption of acetylsalicylic acid onto SILs also are presented in Table 5. Based on these values, two operational stages are identified: the first stage corresponding to the steep-sloped portion of qt vs $t^{1/2}$ plots and the second one resembling the linear gentle-sloped portion, with a breakpoint (square root of the time where the two linear segments intersects). These two stages may correspond to the diffusion process of acetylsalicylic acid in the pores of different sizes and gradually smaller of SILs[49] . The values of K_{id} (Table 5) are in accordance with this assumption, i.e. higher K_{id} values are recorded for the first stage. Furthermore, the higher K_{id} value verified with [Si][N_{3888}]Cl reveals that acetylsalicylic acid diffusion is faster in this SIL.

The relationship between the equilibrium distribution of acetylsalicylic acid between the liquid and solid phases is given by the adsorption isotherms, which are given in Figure 4. The contact time to perform these studies was set at 140 min, to ensure that equilibrium was fully achieved, with concentrations of acetylsalicylic acid ranging from 0.012 to 0.32 g/L.

Table 5. Values corresponding to the piecewise linear regression for the first linear segment in the Boyd plots and of the first two linear segments in the Webber's plot for the acetylsalicylic acid adsorption onto SILs. Values given in brackets correspond to the 95% confidence limits.

		Boyd's film diffusion model	Webber's intraparticle diffusion model	
SIL	Stage	Intercept [lower, upper bound]	Breakpoint ($min^{1/2}$)	K_{id} (mmol/g·$min^{1/2}$) [lower, upper bound]
[Si][C_3C_1im]Cl	1st	0.0002 [-0.00002, 0.00042]	4.00	0.0003 [0.00010, 0.00050]
	2nd			0.0000 [0.00000, 0.000100]
[Si][N_{3114}]Cl	1st	0.0068 [-0.00383, 0.01748]	2.73	0.0016 [-0.0018, 0.0049]
	2nd			0.0001 [0.0000, 0.0002]
[Si][N_{3444}]Cl	1st	0.0005 [-0.00134, 0.00224]	2.63	0.0050 [0.0015, 0.0115]
	2nd			0.0001 [0.0000, 0.0001]
[Si][N_{3888}]Cl	1st	-0.0007 [-0.00487, 0.00342]	1.71	0.0102 [-0.0069, 0.0272]
	2nd			0.0002 [0.0000, 0.0003]

The equilibrium adsorption of acetylsalicylic acid onto SILs increases with the increase of its initial concentration, until saturation is achieved. For all SILs, a plateau is reached at around the q_e value, corresponding to the equilibrium concentration and saturation of the respective material. The existence of a plateau further demonstrates that there is no desorption of acetylsalicylic acid as the concentration increases. Moreover, the relationship between the equilibrium distribution of acetylsalicylic acid between the liquid and solid phases decreases in the following sequence of SILs: [Si][N_{3114}]Cl > [Si][N_{3444}]Cl > [Si][N_{3888}]Cl > [Si][C_3C_1Im]Cl. This sequence is in good agreement with the kinetic results shown in Figure 3.

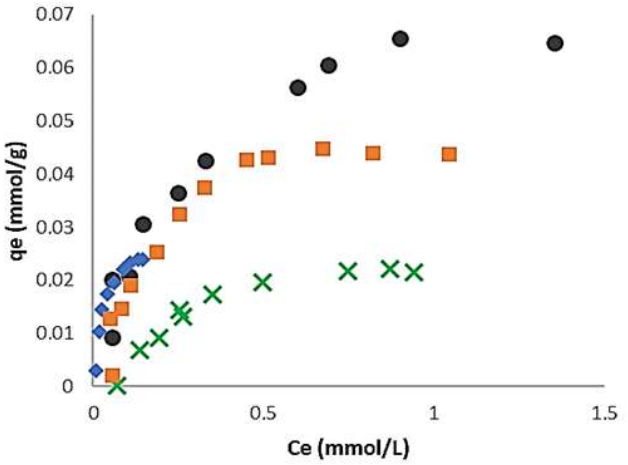

Figure 4. Adsorption isotherms for acetylsalicylic acid onto SILs at 25°C: ×, [Si][C_3C_1Im]Cl; ●, [Si][N_{3114}]Cl; ■, [Si][N_{3444}]Cl; ◆, [Si][N_{3888}]Cl.

The experimental data corresponding to the adsorption isotherms were fitted by the Langmuir[53] and Freundlich[54] models, given by Eqs VI and VII:

$$q_e = \frac{q_{max} \times B \times C_e}{1 + B \times C_e} \quad \text{(VI)}$$

$$q_e = K_f \times C_e^{1/n} \quad \text{(VII)}$$

where C_e is the equilibrium concentration of adsorbate (mmol/L), q_e is the equilibrium concentration of adsorbate in the solid phase (mmol/g), B (L/mmol) is the Langmuir isotherm constant, q_{max} (mmol/g) is the maximum capacity of monolayer coverage, and K_f (adsorption capacity) and n (adsorption intensity) are the constants of the Freundlich equation.

In Table 6 are presented the adsorption isotherms parameters and the respective correlation coefficients (R^2) resulting from the fitting by the Langmuir[53] and Freundlich[54] models. By comparing the values of R^2 of both models, it is shown that the acetylsalicylic acid adsorption onto the four SILs is best described by the Langmuir model. These results reinforce that the adsorption of the pharmaceutical occurs through the formation of a monolayer on the outer surface of the adsorbent, where no further adsorption takes place. Additionally, the relationship between the equilibrium concentrations of acetylsalicylic acid between the solid and liquid phases is best fitted by the Langmuir model for the SIL [Si][N_{3114}]Cl.

Table 6. Correlation coefficients obtained with the Langmuir and Freundlich models for the adsorption isotherms of the adsorbate into the adsorbent (SILs).

	Langmuir model			Freundlich model		
SILs	q_{max} (mmol/g)	B (L/mmol)	R^2	k_f (mmol/g)	n	R^2
[Si][C_3C_1Im]Cl	0.03	2.27	0.967	0.0250	1.83	0.929
[Si][N_{3114}]Cl	0.08	4.03	0.982	0.0612	2.76	0.945
[Si][N_{3444}]Cl	0.06	4.43	0.972	0.0511	2.33	0.925
[Si][N_{3888}]Cl	0.03	27.5	0.986	0.0589	2.35	0.950

A maximum equilibrium concentration (q_{max}) of acetylsalicylic acid of 0.08 mmol (0.014 g) *per* gram of material was obtained with [Si][N_{3114}]Cl. On the other hand [Si][C_3C_1Im]Cl and [Si][N_{3888}]Cl, have the lowest q_{max} values, namely 0.03 mmol of acetylsalicylic acid *per* gram of SIL. These results suggest that the IL chemical structure plays a role in defining the material adsorption

performance. SILs with aromatic character, which is the case of [Si][C_3C_1Im]Cl, do not enhance the adsorption efficiency, meaning that $\pi\cdots\pi$ interactions occurring between the imidazolium ring and acetylsalicylic acid are not relevant. On the other hand, tetraalkylammonium-based SILs with shorter alkyl side chains have a higher adsorption performance. The trend obtained for the tetraalkylammonium-based SILs follows the IL bonding amount (Table 1), reinforcing that the acetylsalicylic acid adsorption depends on the number of IL functional groups. When comparing the number of IL functional groups *per* gram of tetraalkylammonium-based SILs with the number of moles of acetylsalicylic acid at q_{max}, there are 0.08, 0.06, 0.03 moles of IL *per* 0.548, 0.106, 0.051 moles of acetylsalicylic acid in the SILs [Si][N_{3114}]Cl, [Si][N_{3444}]Cl, [Si][N_{3888}]Cl, respectively. These results suggest that each IL functional moiety may interact with 2 to 7 molecules of acetylsalicylic acid that promote the API adsorption. As previously remarked, no functionalized silica has no capacity to adsorb acetylsalicylic acid.

Overall, amongst the studied SILs, [Si][N_{3114}]Cl is the best identified material to remove acetylsalicylic acid from aqueous media. There are some studies in the literature showing the use of different functionalized materials for the removal of acetylsalicylic acid from aqueous solutions. Rakic et al.[43] reported maximum adsorption capacities ranging from 0.011 to 0.021 mmol/g, using a natural zeolite (clinoptilolite) modified with metal cations (Cu (II), Zn (II), Ni (II) and Mn (II)) and with clays (kaolin and bentonite, pure or modified by ion exchange with octadecyldimethylbenzylammonium chloride). Comparing these reported results with those obtained herein, SILs appear as more promising materials for the removal of acetylsalicylic acid (q_{max} value of 0.08 mmol/g). Additionally, 3 types of activated carbon were studied to remove acetylsalicylic acid from aqueous solutions, with a reported q_e of 0.1 mmol/g[42], being this value similar to our best reported result. Despite the similar results it should be noted that the use of activated carbon presents some concerns, particularly in what concerns its disposal after treatment and high operating costs for its recycling[44]. The SILs regeneration and reuse was previously demonstrated[44]. Among several solvents investigated, the mixture composed of 1-butanol and water (85:15, v:v) was identified as the most promising and eco-friendly to regenerate SILs. Given the SILs similarity it is expected that the ones prepared in this work could be recycled as well.

Acetylsalicylic acid is found in effluents in µg/L levels, with a reported maximum value of 1.5 µg/L in water treatment plants[55]. Considering a value of 1 µg/L, and a maximum adsorption capacity of 0.08 mmol/g, it can be envisioned that 1 g of the best material ([Si][N_{3114}]Cl) will be able to treat ca. 14,500 L of water under "ideal" conditions.

SILs cytotoxicity evaluation

Envisioning their potential use for water treatment, the cytotoxicity of the different SILs was assessed using the human hepato cellular carcinoma (HepG2) cell line. This liver cell line was selected since it is the most commonly used cell line for drug metabolism and toxicity studies of chemicals and drugs[56,57].

Cells were exposed during 24h to the cell culture medium that was previously in contact with the different SILs (0.25g of material/L) for 30 min and 120 min. These two contact times were chosen based on the potential to use these materials for tap water and effluents treatment. The results obtained were normalized to the control (untreated cells), and are shown in Figure 5.

Amongst the tested materials, for a contact time of 30 min, [Si][N_{3114}]Cl and [Si][N_{3444}]Cl are the less toxic ones, with cell viability results close to 100%, whereas [Si][C_3C_1Im]Cl is the most toxic, followed by [Si][N_{3888}]Cl. The higher toxicity of the imidazolium-based SIL is expected, as this class of IL is generally recognized as being more cyto- and eco-toxic due to the presence of an aromatic ring[58–60]. Nevertheless, even for this SIL the decrease in cell viability was lower than 30%. Previous reports disclosed the high toxicity of 1-hexadecyl-3-methylimidazolium chloride and 1-dodecyl-3-methylimidazolium chloride towards HepG2 cells[60,61]. The low toxicity observed in SILs comprising imidazolium suggest that it is not bioavailable for the cells and that the IL leaching is not occurring. For the tetraalkylammonium-based SILs, ILs with longer alkyl side chains lead to higher eco- and cytotoxicity due to their higher ability to penetrate phospholipidic membranes[62]. For [Si][N_{3888}]Cl, a maximum decrease of 22% in the cell viability occurs after 30 min of contact, which is in line with the value obtained for [Si][C_3C_1im]Cl. Furthermore, the results for cell viability closely follow the ones obtained for the material adsorption efficiency for acetylsalicylic acid ([Si][N_{3114}]Cl > [Si][N_{3444}]Cl > [Si][N_{3888}]Cl > [Si][C_3C_1Im]Cl), with the less toxic materials displaying the best results in terms of removal efficiency, which is an additional advantage when considering the best material to use as an alternative adsorbent. Expecting that a higher number of IL functional groups would be more toxic, this tendency on the cells viability also demonstrates that it is not the number of IL functional groups that defines the cells viability, but instead the IL chemical structure.

Overall, most studied SILs do not show a significant decrease on the cell's viability after being in contact for 30 min and 120 min with the material. Remarkably, the best identified material to remove acetylsalicylic acid from aqueous solutions ([Si][N_{3114}]Cl) does not induce any decrease in cell viability, opening new and exciting possibilities for its use on the removal of this pharmaceutical (and others) from water samples, such as effluents from wastewater treatment plants and hospitals, and even drinking water.

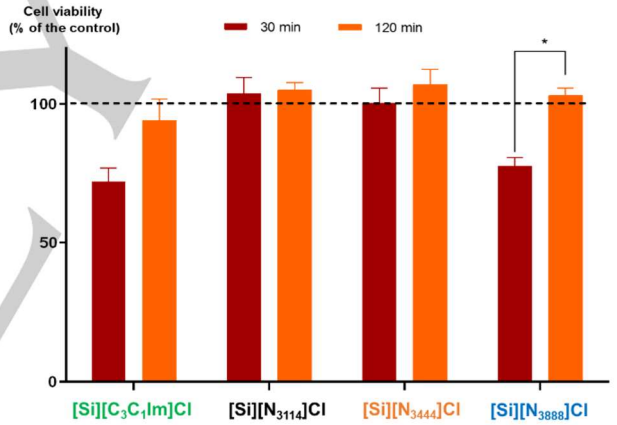

Figure 5. HepG2 cell viability after 24 h exposure to the culture medium incubated for 30 min (brown bars) and 120 min (orange bars) with the different materials. The dotted line represents the control (untreated cells). The results presented (average and standard error) refer to three independent experiments with five replicates per experiment. The (*) indicates significant differences ($p<0.05$).

Conclusion

In the current work, four supported IL-based silica materials were synthesized and characterized, namely [Si][N_{3114}]Cl, [Si][N_{3444}]Cl, [Si][N_{3888}]Cl and [Si][C_3C_1Im]Cl. The IL functionalization was demonstrated by solid-State ^{13}C nuclear magnetic resonance spectroscopy, FTIR and elemental analysis.

The potential of the prepared SILs as alternative adsorbents to remove pharmaceuticals from water was appraised with acetylsalicylic acid, one of the most used pharmaceuticals, by determining the respective adsorption kinetics and isotherms. It was found that the number of IL functional groups is not relevant when comparing the imidazolium- with the tetraalkylammonium-based SILs, meaning that the IL chemical structure plays a more

significant role in defining the materials adsorption performance. The most efficient material for the removal of acetylsalicylic acid from aqueous solutions is [Si][N_{3114}]Cl, with a maximum adsorption capacity of 0.08 mmol of acetylsalicylic acid *per* gram of material. Accordingly, under ideal conditions, 1 g of this material is sufficient to treat ca. 14,500 L of water containing 1 µg/L of acetylsalicylic acid.

Envisioning the use of SILs to treat drinking water, their cytotoxicity towards human hepato cellular carcinoma (HepG2) cell line was evaluated. Most SILs display a negligible toxicity towards the studied cell line, with the best SIL identified, [Si][N_{3114}]Cl, not inducing any decrease in cell viability. The obtained results show the possibility of using SILs as effective materials to remove acetylsalicylic acid from water, paving the way for their use to remove other pharmaceuticals of environmental concern, and that could be ideally applied as novel materials to treat aqueous samples such as effluents and even drinking water.

Experimental Section

Materials and Methods. The reagents used for the SILs synthesis were: (3-chloropropyl)trimethoxysilane, tributylamine and N-methylimidazole, purchased from Acros Organics (>98% pure); N,N-dimethylbutylamine (99% pure) and Hydrochloric acid (ACS reagent, 37%) acquired from Sigma Aldrich; trioctylamine (<98% pure) from Fluka; and toluene (>99.5 % pure), acquired from Fisher Chemical. Ethanol (purity 99.9 %) and methanol (HPLC grade) were acquired from Carlo Erba and Chem-Lab, respectively. The starting silica gel particles (60Å) were acquired from Merck. Acetylsalicylic acid (99.9%) was obtained from Sigma Aldrich. For cytotoxicity tests the cell counting kit-8 (CCK-8) was purchased from Dojindo Molecular Technologies, the antibiotics (penicillin and streptomycin) from Gibco, the HepG2 expansion media from Celleng-tech and Fetal Bovine Serum (FBS) from Merck Millipore. The collagen-coated 96-well plates from Zenbio and the in bovine collagen coated flask from Greiner bio-one.

Preparation of Supported Ionic Liquids. Commercial silica gel, with a pore size of 60 Å, was used as a starting material for the SILs synthesis. The used procedure follows the one published by Qiu et al.[45], with some adjustments. As a first step, silica was activated with a strongly acidic aqueous solution, hydrochloric acid (37%, w/w), for 24 h, in order to enhance the content of silanol groups on the silica surface. Afterwards, the activated silica particles were washed with distilled water and dried at 60°C for 24 h. 60 mL of toluene were then added to activated silica (5.0 g) and 5 mL of 3-chloropropylmethoxysilane, in order to obtain chloropropyl silica ([Si][C_3]Cl). The suspension was refluxed under magnetic stirring for 24 h. The obtained material was filtered and washed with toluene (100 mL), 1:1 ethanol:water mixture (200 mL), distilled water (500 mL) and methanol (100 mL), and finally dried at 60°C for 24 h. The prepared material ([Si][C_3]Cl) was added to 50 mL of toluene and 5 mL of 1-methylimidazole or other reagents as the source of the cation (N,N-dimethylbutylamine, tributylamine or trioctylamine, see Scheme 1). The prepared suspension was magnetically stirred under reflux for 24 h. The obtained materials were filtered and washed with toluene (100 mL), methanol (350 mL), distilled water (300 mL) and methanol (150 mL), and then dried at 60°C for 24 h.

SILs Characterization. The prepared SILs were characterized by elemental analysis, specific surface area (S_{BET}), solid-State ^{13}C nuclear magnetic resonance (NMR) spectroscopy, FTIR spectroscopy, Point Zero Charge (PZC) and Scanning Electron Microscopy (SEM).

The content (weight percentage) of carbon, hydrogen and nitrogen in the synthetized SILs ([Si][C_3C_1Im]Cl, [Si][N_{3114}]Cl, [Si][N_{3444}]Cl, [Si][N_{3888}]Cl) was determined by elemental analysis using a TruSpec 630-200-200 CHNS analyser. A sample of ca. 2 mg was introduced into the apparatus at a combustion furnace temperature of 1075°C and an afterburner temperature of 850°C. Infrared absorption was used to determine the carbon and hydrogen contents whereas thermal conductivity was used for nitrogen quantification.

The specific surface area (S_{BET}) of silica and SILs were evaluated by gas adsorption using a Gemini V-2380 surface area analyzer (Micromeritics, Norcross, GA, USA) and determined by the Brunaer–Emmett–Teller (BET) equation with multipoint adsorption isotherms of N_2 at -196ºC. Prior to the measurements, the samples were degassed overnight at 100ºC.

Solid-State ^{13}C nuclear magnetic resonance (NMR) spectroscopy was used to confirm the SILs preparation. ^{13}C NMR spectra were recorded at 9.7 T on a using 4 mm BL cross-polarization magic angle spinning (CPMAS) VTN probes at 100.6 MHz, at room temperature.

Zeta potential values were recorded in a Malvern Zetasizer Nano ZS (Malvern Instruments Ltd. Malvern) using several suspensions of the prepared materials in water at different pH values. In order to adjust the pH values, solutions of NaOH and HCl (0.01 M) were used, and measurements were carried at 25°C using a cell suitable for this purpose.

Scanning electron microscopy (SEM) was performed using a Hitachi SU-70 microscope equipped with EDX Bruker, model Quantax 400. A carbon thin film deposition was used to increase the conductivity of the samples.

Adsorption kinetics and isotherms. The adsorption kinetics of acetylsalicylic acid in each SIL were initially determined in order to address the adsorption behavior and time required for equilibrium. 10 mL of aqueous solutions of acetylsalicylic acid with a concentration of 0.032 g/L (0.178 mmol/L) were used, while keeping the weight of each SIL constant (0.064 g). These solutions and each SIL were placed on an orbital shaker at 150 rpm and at (25 ± 0.5)°C. Samples were collected between 0 and 180 min. Solutions were centrifuged at 6000 rpm for 10 min and the supernatants were collected for the quantification of acetylsalicylic acid. At least two replicates were performed for each time. The equilibrium concentration of adsorbate in the solid phase (*q*e, mmol/g) was determined according to (Equation VIII):

$$q_e = \frac{(C_0 - C_e) \times V}{w} \qquad \text{(VIIVIII)}$$

where *w* is the weight of SIL (g), *V* is the volume of the aqueous solution containing the target pharmaceutical (L), and *C*0 and *Ce* are the equilibrium concentrations of acetylsalicylic acid before and after adsorption onto SILs, respectively (mmol/L).

To determine the adsorption isotherms of acetylsalicylic acid in the studied SILs, different concentrations of acetylsalicylic acid, ranging from 0.012 to 0.32 g/L, were used. After 140 min of agitation, at the same conditions as previously described, solutions were centrifuged and the supernatants collected for the quantification of the target pharmaceutical.

The adsorption efficiency of (% AE) of acetylsalicylic acid onto SILs, for a given concentration of pharmaceutical and weight of SIL, was determined according to the following equation:

$$\%AE = \left(\frac{C_0 - C_e}{C_0}\right) \times 100 \qquad \text{(IX)}$$

where C_0 and C_e are the equilibrium concentrations of acetylsalicylic acid before and after adsorption onto SILs, respectively (in mmol/L). The initial concentration of acetylsalicylic acid in these studies was 0.178 mmol/L, and the weight of each SIL was kept constant at 0.064 g.

The quantification of acetylsalicylic acid was performed by UV-Vis spectroscopy using a Shimadzu UV-1800, Pharma-Spec UV-Vis, and 1x1cm quartz cells. A calibration curve was established at the maximum wavelength of acetylsalicylic acid (273 nm).

Cytotoxicity studies. Human *hepatoma* cell line Hep G2 ([HEPG2] (ATCC® HB-8065™)) was used to evaluate the potential cytotoxicity of [Si][C_3C_1im]Cl, [Si][N_{3114}]Cl, [Si][N_{3444}]Cl and [Si][N_{3888}]Cl. Cells were cultured in Bovine Collagen Coated Flask 75 cm^2 growth area with HepG2 Expansion Media (HEPG2.E.MEDIA) with 10% (v/v) fetal bovine serum (FBS) and 0.1% penicillin/streptomycin, and were maintained at 37°C in a humidified atmosphere of 5% CO_2. For the experiments, HepG2 cells from low passages (P5-P9) were trypsinized with trypsin/EDTA solution at approximately 70-80% of confluence. These cells were plated in collagen-coated 96-well plates with a density of 1x10^4 cells/well. After 48 h, cells were exposed to the culture medium previously exposed to the materials (0.25g/L) at 2 contact times: 30 and 120 min. Considering that the materials were not sterile, the medium was passed through a 0.22 µm sterile filter inside a laminar flow cabinet. The control was also passed through the same type of filter. Cells were exposed in collagen-coated wells to the stimulus for 24 h, after which, cell viability was assessed using the CCK-8 (Cell Counting Kit-8) kit. This kit determines the number of viable cells in cell proliferation and cytotoxicity assays. It is based on the principle that, in live cells, the dehydrogenases are able to reduce the water soluble tetrazolium salt WST-8 ([2-(2-methoxy-4-nitrophenyl)-3-(4-nitrophenyl)-5-(2,4-disulfophenyl)-2H-tetrazolium, monosodium salt]) into a water-soluble formazan dye, giving rise to an orange product and thus its absorbance can be quantified in a microplate spectrophotometer (xMArkTM Microplate Absorbance Spectrophotometer, BIO-RAD, absorbance measured at 450 nm).

Cell viability was calculated based on the relative absorbance compared with the control group (unexposed cells). For each material, a minimum of three independent assays of five replicates were performed. Differences between the two contact times were determined using the Bonferroni-

Dunn method, with a significance level of 0.05. Cell proliferation results between the different materials were compared using one-way ANOVA. The significance level was set at 0.05.

Acknowledgements

This work was developed within the scope of the project CICECO-Aveiro Institute of Materials, UIDB/50011/2020 & UIDP/50011/2020, financed by national funds through the Portuguese Foundation for Science and Technology/MCTES. The NMR spectrometers used in this work are part of the National NMR Network (PTNMR) and are partially supported by Infrastructure Project Nº 022161 (co-financed by FEDER through COMPETE 2020, POCI and PORL and FCT through PIDDAC. This work was financially supported by the project POCI-01-0145-FEDER-031106 (IonCytDevice) funded by FEDER, through COMPETE2020—Programa Operacional Competitividade e Internacionalização (POCI), and by national funds (OE), through FCT/MCTES, and developed in the scope of the "Smart Green Homes" Project [POCI-01-0247-FEDER-007678], a co-promotion between Bosch Termotecnologia S.A. and the University of Aveiro. It is financed by Portugal 2020 under the Competitiveness an Internationalization Operational Program, and by the European Regional Development Fund. Márcia C. Neves acknowledges FCT, I.P. for the research contract CEECIND/00383/2017 under the CEEC Individual 2017; Sandra C. Bernardo acknowledges FCT for the research contract under the project POCI-01-0145-FEDER-029496; and Ana C.A. Sousa acknowledges Universidade de Aveiro for funding in the scope of the framework contract foreseen in the numbers 4, 5, and 6 of the article 23, of the Decree-Law 57/2016, of August 29, changed by Law 57/2017, of July 19.

Keywords: Acetylsalicylic acid • Functionalized Silica • Supported Ionic Liquids • Adsorption • Kinetics• Isotherms

References

[1] T. aus der Beek, F.-A. Weber, A. Bergmann, S. Hickmann, I. Ebert, A. Hein, A. Küster, *Environ. Toxicol. Chem.* **2016**, *35*, 823–835.
[2] K. Klaus, *Annu. Rev. Environ. Resour.* **2010**, *35*, 57–75.
[3] Q. Fu, T. Malchi, L. J. Carter, H. Li, J. Gan, B. Chefetz, *Environ. Sci. Technol.* **2019**, *53*, 14083–14090.
[4] A. Küster, N. Adler, *Philos Trans R Soc L. B Biol Sci.* **2014**, *369*, 20130587.
[5] R. Rosal, A. Rodríguez, J. A. Perdigón-Melón, A. Petre, E. García-Calvo, M. J. Gómez, A. Agüera, A. R. Fernández-Alba, *Water Res.* **2010**, *44*, 578–588.
[6] A. B. A. Boxall, M. A. Rudd, B. W. Brooks, D. J. Caldwell, *Environ. Health Perspect.* **2012**, *120*.
[7] K. E. Arnold, A. R. Brown, G. T. Ankley, J. P. Sumpter, *Philos Trans R Soc L. B Biol Sci.* **2014**, *369*, 20130569.
[8] M. de Oliveira, F. E. B. Frihling, J. Velasques, F. J. C. M. Filho, P. S. Cavalheri, L. Migliolo, *Sci. Total Environ.* **2020**, *705*, 135568.
[9] E. Touraud, B. Roig, J. P. Sumpter, C. Coetsier, *Int. J. Hyg. Environ. Health* **2011**, *214*, 437–441.
[10] K. Kümmerer, A. Al-ahmad, B. Bertram, M. Wiessler, *Chemosphere* **2000**, *40*, 767–773.
[11] J. Besse, J. Latour, J. Garric, *Environ. Int.* **2012**, *39*, 73–86.
[12] J. Zhang, V. W. C. Chang, A. Giannis, J. Wang, *Sci. Total Environ.* **2013**, *445–446*, 281–298.
[13] M. Cesen, T. Elersek, M. Novak, B. Zegura, T. Kosjek, M. Filipic, E. Heath, *Environ. Pollut.* **2016**, *210*, 192–201.
[14] B. Kasprzyk-hordern, R. M. Dinsdale, A. J. Guwy, *Water Res.* **2009**, *43*, 363–380.
[15] C. G. Daughton, in *Pharm. Care Prod. Environ.* (Ed.: T.L.J.-L. Christian G. Daughton), American Chemical Society, **2009**, p. Volume 791, Chapter 1, pp 2–38.
[16] Z. Chen, G. Park, P. Herckes, P. Westerhoff, *J. Adv. Oxid. Technol.* **2008**, *11*, 254–260.
[17] L. F. Delgado, V. Faucet-marquis, A. Pfohl-leszkowicz, C. Dorandeu, B. Marion, S. Schetrite, C. Albasi, *Bioresour. Technol.* **2011**, *102*, 4395–4401.
[18] L. Kovalova, H. Siegrist, H. Singer, A. Wittmer, C. S. Mcardell, *Environ. Sci. Technol.* **2012**, *46*, 1536−1545.
[19] L. A. Fernández, C. Hernández, M. Bataller, E. Véliz, A. López, O. Ledea, S. Padrón, *Water Environ. J.* **2010**, *24*, 174–180.
[20] V. Matamoros, J. Bayona, *Environ. Sci. Technol.* **2006**, *40*, 5811–5816.
[21] B. I. Escher, W. Pronk, M. J.-F. Suter, M. Maurer, *Environ. Sci. Technol.* **2006**, *40*, 5095–5101.
[22] N. Fontanals, S. Ronka, F. Borrull, A. W. Trochimczuk, R. M. Marcé, *Talanta* **2009**, *80*, 250–256.
[23] T. D. Ho, A. J. Canestraro, J. L. Anderson, *Anal. Chim. Acta* **2011**, *695*, 18–43.
[24] L. Vidal, M. Riekkola, A. Canals, *Anal. Chim. Acta* **2012**, *715*, 19–41.
[25] N. Fontanals, F. Borrull, R. M. Marcé, *Trends Anal. Chem.* **2012**, *41*, 15–26.
[26] M. G. Freire, A. F. M. Cláudio, J. M. M. Araújo, J. A. P. Coutinho, I. M. Marrucho, J. N. C. Lopes, L. P. N. Rebelo, *Chem. Soc. Rev.* **2012**, *41*, 4966–4995.
[27] L. Dai, S. Yu, Y. Shan, M. He, *Eur. J. Inorg. Chem.* **2004**, 237-241.
[28] C. Cesari, A. Cingolani, M. Teti, A. Messori, S. Zacchini, V. Zanotti, R. Mazzoni, *Eur. J. Inorg. Chem.* **2019,** *11-12*, 1114-1122.
[29] L. Vidal, J. Parshintsev, K. Hartonen, A. Canals, M.-L. Riekkola, *J. Chromatogr. A* **2012**, *1226*, 2–10.
[30] D. Bratkowska, N. Fontanals, S. Ronka, A. W. Trochimczuk, F. Borrull, R. M. Marcé, *J. Sep. Sci.* **2012**, *35*, 1953–1958.
[31] J. C. Moreira, Y. Gushikem, *Anal. Chim. Acta,* **1985**, *176*, 263–267.
[32] X. H. J. Shu, F. Liu, X. Zhou, S. X. Jiang, X. Liu, L. Zhao, *Chin. Chem. Lett.* **2004**, *15*, 1060–1062.
[33] M. J. R. Desborough, D. M. Keeling, *Br. J. Haematol.* **2017**, *177*, 674–683.
[34] J. Ma, Z. Cai, H. Wei, X. Liu, Q. Zhao, T. Zhang, *Biomed. Pharmacother. J.* **2017**, *95*, 656–661.
[35] M. Cleuvers, *Ecotoxicol. Environ. Saf.* **2004**, *59*, 309–315.
[36] M. N. Mons, A. C. Hogenboom, T. H. M. Noij, *Pharmaceuticals and Drinking Water Supply in the Netherlands*, Nieuwegein : KIWA Water Research, **2003**.
[37] M. Stumpf, T. A. Ternes, R.-D. Wilken, S. V. Rodrigues, W. Baumann, *Sci. Total Environ.* **1999**, *225*, 135–141.
[38] M. Papageorgiou, I. Zioris, T. Danis, D. Bikiaris, D. Lambropoulou, *Sci. Total Environ.* **2019**, *694*, 133565.
[39] D. Camacho-Muñoz, Julia Martín, J. L. Santos, I. Aparicio, E. Alonso, *Chemosphere* **2014**, *111*, 70–79.
[40] E. Carmona, V. Andreu, Y. Picó, *Sci. Total Environ.* **2014**, *484*, 53–63.
[41] P. Paíga, L. H.M.L.M.Santos, S. Ramos, S. Jorge, J. G. Silva, C. Delerue-Matos, *Sci. Total Environ.* **2016**, *573*, 164–177.
[42] V. Rakic, V. Rac, M. Krmar, O. Otman, A. Auroux, *J. Hazard. Mater. j* **2015**, *282*, 141–149.
[43] V. Rakic, N. Rajic, A. Dakovic, A. Auroux, *Microporous Mesoporous Mater.* **2013**, *166*, 185–194.
[44] H. F. D. Almeida, M. C. Neves, T. Trindade, I. M. Marrucho, M. G. Freire, *Chem. Eng. J.* **2020**, *381,* 122616.
[45] H. Qiu, S. Jiang, X. Liu, *J. Chromatogr. A* **2006**, *1103*, 265–270.
[46] S. Y. Lagergren, *thesis* **1898**.
[47] Y. S. Ho, G. McKay, *Process Biochem.* **1999**, *34*, 451–465.
[48] J.-P. Simonin, *Chem. Eng. J.* **2016**, *300*, 254–263.
[49] M. I. El-Khaiary, G. F. Malash, *Hydrometallurgy* **2011**, *105*, 314–320.
[50] G. F. Malash, M. I. El-Khaiary, *Chem. Eng. J.* **2010**, *163*, 256–263.

[51] G. E. Boyd, A. W. Adamson, L. S. Myers Jr., *J. Am. Chem. Soc.* **1947**, *69*, 2836–2848.
[52] W. J. Weber, J. C. Morris, *J. Sanit. Eng. Div. Proc. Am. Soc. Civ. Eng.* **1963**, *89*, 31–59.
[53] I. Langmuir, *J. Am. Chem. Soc.* **1918**, *40*, 1361–1403.
[54] H. Freundlich, *Zeitschrift für Phys. Chemie* **1907**, *57U*.
[55] T. A. Ternes, *Water Res.* **1998**, *32*, 3245–3260.
[56] M. T. Donato, L. Tolosa, M. J. Gómez-Lechón, in *Methods Mol. Biol. (Methods Protoc.* (Eds.: M. Vinken, V. Rogiers), **2015**.
[57] S. Knasmüllera, V. Mersch-Sundermann, S. Kevekordes, F. Darroudid, W. . Huber, C. Hoelzl, J. Bichler, B. . Majer, *Toxicology* **2004**, *198*, 315–328.
[58] F. A. e Silva, J. A. P. Coutinho, S. P. M. Ventura, *Encycl. Ion. Liq.* **2019**.
[59] G. Chatel, E. Naffrechoux, M. Draye, *J. Hazard. Mater.* **2017**, *324*, 773–780.
[60] R. Wan, X. Xia, P. Wang, W. Huo, H. Dong, Zhongjie Chang, *Toxicol. Vitr.* **2018**, *52*, 1–7.
[61] P. Wang, R. Wan, W. Huo, H. Dong, Z. Chang, X. Xia, *Environ. Toxicol.* **2020**.
[62] S. P. M. Ventura, A. M. M. Gonçalves, T. Sintra, J. L. Pereira, F. Gonçalves, J. A. P. Coutinho, *Ecotoxicology* **2013**, *22*, 1–12.

Entry for the Table of Contents

New materials based on silica functionalized with ionic liquids (SILs) were synthetized and characterized aiming their use in the removal of pharmaceuticals from aqueous samples. The obtained results disclose that the best SIL has high capacity for the adsorption/removal of acetylsalicylic acid, with no negative cytotoxic impacts towards human cell lines, reinforcing its potential to treat water samples.

Key topic: Pharmaceuticals removal.